Translational Medicine Communications

RESEARCH

Open Access

Imaged-guided focused ultrasound in combination with various formulations of doxorubicin for the treatment of diffuse intrinsic pontine glioma

Rianne Haumann[1,2], John I. Bianco[1,2], Piotr M. Waranecki[1,2], Pieter J. Gaillard[3], Gert Storm[4,5], Mario Ries[6], Dannis G. van Vuurden[1,2], Gertjan J. L. Kaspers[1,2] and Esther Hulleman[1,2*]

Abstract

Background: Diffuse intrinsic pontine glioma (DIPG) is a notoriously difficult tumor to treat, with an overall survival of DIPG patients being only 11 months. One of the major obstacles for the effective treatment of DIPG is the blood–brain barrier (BBB). In order to circumvent the BBB, drug delivery methods are needed that target the pontine area. One such approach is microbubble-mediated focused ultrasound (FUS)—a non-invasive method that can temporarily and locally open the BBB. Previously, it was shown that FUS is safe with minimal side effects and rapid recovery times in preclinical animal models with different DIPG tumors. However, recent studies have shown that combining FUS with a single treatment of the chemotherapeutic drug doxorubicin did not improve survival in a DIPG xenograft model. As the duration of doxorubicin exposure might play a role in tumor response, we hypothesized that the use of a long-circulation (PEGylated) liposomal formulation of doxorubicin could lead to improved overall survival through a longer exposure time to the tumor.

Method: DIPG xenograft models were established with orthotopic injections of HSJD-DIPG-07 tumor cells into the pontine area of female athymic nude-foxn1^{nu} mice. Tumor engraftment was confirmed with bioluminescence imaging (BLI) 40 days post-inoculation. Mice were randomized into groups receiving either liposomal formulations of doxorubicin (2B3-101 or Caelyx®) or free doxorubicin in combination with or without FUS treatment. Treatment groups received 5 mg/kg 2B3-101 or Caelyx® 1 h before FUS treatment or 5 mg/kg free doxorubicin immediately after FUS.

Results: Histological analysis, however, revealed liposome extravasation in healthy controls but not in HSJD-DIPG-07 xenograft 24 h after treatment. Furthermore, BLI monitoring did not show reduced signal after treatment, which was further illustrated with a survival analysis, showing no significant difference between treated and control animals ($p = 0.3$).

Conclusion: We did not observe a treatment effect after a single dose of free doxorubicin or the liposomal formulations 2B3-101 or Caelyx® in combination with FUS in DIPG-bearing mice.

*Correspondence: E.Hulleman@prinsesmaximacentrum.nl
[1] Princess Máxima Center for Pediatric Oncology, Heidelberglaan 25, 3584 CS Utrecht, The Netherlands
Full list of author information is available at the end of the article

Keywords: Diffuse intrinsic pontine glioma, Focused ultrasound, Blood–brain barrier, Liposomes, Nanomedicine, Doxorubicin, Drug delivery

Background

Diffuse intrinsic pontine glioma (DIPG) is an aggressive, inoperable pediatric brain tumor with very limited and ineffective treatment options outside radiation therapy. Neoadjuvant or adjuvant systemic therapy in combination with radiotherapy only prolongs survival for several months [1–3]. With an overall survival of only 11 months, new drug delivery methods are needed to increase the selective tumor exposure to chemotherapeutic drugs. Several attributes exacerbate the poor prognosis of DIPG, including location and maintained integrity of the blood–brain barrier (BBB) [4, 5]. The BBB is a major obstacle for the efficacy of chemotherapeutics in the treatment of brain tumors as it prevents most large molecules to readily enter the brain parenchyma, resulting in the low efficacy of most chemotherapeutics [6]. As only 2% of small molecules (< 500 Da) are able to passively cross the BBB, effective drug delivery methods that increase the exposure of drugs in the brain parenchyma are urgently needed [6]. There are several methods to circumvent or temporarily open the BBB, including the use of nanoparticles, convection enhanced delivery (CED), intranasal, and intra-arterial drug delivery [7, 8]. Although encouraging results have been seen, to date these methods have not led to a significant increase in the treatment of several brain tumors, including gliomas.

DIPGs in particular maintain an intact BBB and thus limited penetration and effectiveness of therapeutics, in comparison to glioblastoma which has a heterogenous BBB with regions of necrosis harbouring areas with both a disrupted and intact BBB [4, 5, 9]. Since DIPG resides in the pons, a fragile and inoperable structure of the brain, a non-invasive method of delivery is preferred.

Focused ultrasound (FUS) is a non-invasive method that can temporarily and locally open the BBB in a reversible fashion [10, 11]. FUS has been used both preclinically and clinically in growing numbers of clinical trials for the treatment of adult gliomas [12–16]. Previous research has shown that FUS can be safely used in a xenograft model of DIPG to effectively open the BBB and increase the passage of chemotherapeutics such as doxorubicin to the targeted area [14, 16]. Although the use of doxorubicin in these experiments did not lead to significant improvement of survival in vivo, doxorubicin was shown to be effective against several patient-derived DIPG cell lines in preclinical studies [16, 17], and lack of efficacy in vivo could have been caused by multiple dose toxicities [14]. To reduce toxicity of systemic administration, liposomal formulations of doxorubicin can be employed [18, 19]. Caelyx® and 2B3-101 are liposomes loaded with doxorubicin which are 80–100 nm large vesicles that have a long plasma-halflife due to polyethylene glycol (PEG) coating. 2B3-101 liposomes have been shown to have a better brain distribution compared to non-targeted PEG liposomal doxorubicin [20, 21] because they are conjugated with the brain-targeting ligand glutathione (GSH). Both liposomal formulations release the drug over a prolonged period of time reducing toxicity [20, 22]. We hypothesize that the use of FUS in combination with liposomal formulations of doxorubicin – that are less toxic and expose the tumor over a prolonged period through sustained release – may have a significant effect in prolonging survival in a preclinical DIPG mouse model. Furthermore, we aimed to investigate the difference between Caelyx® and the 2B3-101 in combination with FUS. Here we describe the use of FUS in combination with free doxorubicin and liposomal formulations of doxorubicin in a HSJD-DIPG-07 xenograft model. We show that treatment with both free and liposomal doxorubicin is safe and well tolerated. However, single treatment did not significantly improve survival in the treatment groups, possibly due to the lack of sustained tumor exposure, even after the application of FUS. The results of this study will contribute to increased knowledge for the use of FUS for the treatment of DIPG and to advice physicians on clinical trials.

Materials and methods

Cell culture

DIPG cell line HSJD-DIPG-07 harboring H3F3A K27M and ACVR1 mutations was kindly provided by Dr. Ángel Montero Carcaboso (Hospital San Joan de Déu Barcelona, Spain). This cell line was transduced with the green fluorescent marker ZsGreen and luciferase as described in Meel et al. [23]. Cells were cultured in tumor stem medium (TSM; 50% DMEM-F12/50% Neurobasal-A, Gibco, UK) base supplemented with penicillin–streptomycin (100 U/ml, PAA Laboratories GmbH, Austria), 1X B27 supplement (without vitamin A, Thermo Fisher, Waltham, MA, USA), 20 ng/ml human basic fibroblast growth factor (bFGF, Peprotech, London, UK), 20 ng/ml human epidermal growth factor (EGF, Peprotech, London, UK), 10 ng/ml human platelet-derived growth factor-AA (PDGF-AA, Peprotech, London, UK), 10 ng/ml human platelet-derived growth factor-BB (PDGF-BB, Peprotech, London, UK), and 2 µg/ml heparin (Vrije

University Medical Center Pharmacy, Amsterdam, The Netherlands) [23]. Short tandem repeat (STR) analysis was used for validation of the cell line. Before use, tumor cells were harvested, mechanically dissociated with accutase and washed with phosphate buffered saline (PBS, Fresenius Kabi GmbH, Graz Austria). Luciferase expression was assessed with a luminometer (Lumat, Berthold Technologies GmbH & Co KG, Bad Wildbad, Germany).

Xenograft model

Animal experiments were conducted in accordance with Dutch national regulation guidelines on animal experimentation, as well as with EU Directive 2010/63/EU. The protocol was approved by the committee on animal experimentation of the Vrije University (VU) (AVD114002017841). Female athymic nude-foxn1nu mice (total $n=69$: $n=63$ with xenograft and $n=6$ without xenograft), 6 weeks of age (Envigo-Harlan Laboratories, Horst, The Netherlands), were kept under filter top conditions with a 12 h artificial light/dark cycle. Mice received food and water ad libitum. Prior to surgery ($n=63$), mice received 0.067 mg/ml of carprofen (Rimadyl®, Zoetis, Rotterdam, The Netherlands) in drinking water for 24 h. Thirty minutes prior to intracranial injection (i.c.) mice received 0.05–0.1 mg/kg of buprenorphine hydrochloride (Temgesic®, Indivior UK Ltd, Berkshire, United Kingdom). Anesthesia was induced with isoflurane (1–3% and 2 l/min of O2, Zoetis, Rotterdam, The Netherlands) and mice were fixed in a stereotactic frame. The depth of anesthesia was determined by the absence of palpebral, withdrawal, and corneal reflexes. Topical administration of 2% of lidocaine was applied before incision along the midline, after which a burr hole was drilled 1.0 mm lateral and 0.8 mm posterior to the lambda using a high-speed drill. A Hamilton syringe (Hamilton Company, Reno, NV, USA) was used to inject 5 µl of 5×10 [5] HSJD-DIPG-07 cells in PBS into the pons at a depth of 4.5 mm, with an infusion rate of 2 µl/min. After injection, the needle was left in place for 2 min before being slowly removed to avoid a vacuum and cell accumulation into the needle tract. The wound was then closed using topical skin adhesive (Dermflex, Vygon, Ecouen, France) and the animals were allowed to awaken under a heating lamp. All animals awoke within 15 to 30 min following surgery and did not present any signs of distress. Carprofen in drinking water was removed 24 h following surgery. Mice received supplemented food (Nutrigel, Portland, ME, USA) for 24 to 48 h after treatment. Mice were regularly weighted and neurologically assessed [24]. Neurological assessment was based on motor score (ranging from no deficit to walking with obvious asymmetry to no movements) and abnormal movements such as tilted head and axial body rotation. Bioluminescence imaging (BLI) was performed once a week to monitor the growth rate of the orthotopic tumors. For BLI, mice were intraperitoneally (i.p.) injected with 150 µl of D-luciferin Potassium Salt (100 mM solution in PBS, Goldbio, St. Louis, MO, USA) 10 min before imaging. Animals were anaesthetized with isoflurane (3% and 2 l/min O2) 5 min prior to imaging. BLI was performed with a Bruker In-Vivo Extreme Capture System (Bruker Corporation, Billerica, MA, USA) with an exposure time of 30 s. For each mouse, a region of interest (ROI) defined the luminescent area of the tumor and the mean intensity of the ROI (photon/sec/m2) was calculated using Molecular Imaging Software (Bruker Corporation, Billerica, MA, USA).

Focused ultrasound

The imaged-guided focused ultrasound method was previously described in Haumann et al. [25]. In brief, mice received 0.05–0.1 mg/kg of buprenorphine 15–30 min before anesthesia with isoflurane (1–3% and 2 l/min of O_2). The depth of anesthesia was determined by the absence of palpebral, withdrawal, and corneal reflexes. A 26 G catheter (Neoflon, Becton Dickinson, Helsingborg, Sweden) was placed in the tail vein and flushed with 50 UI of heparin (Vrije University Medical Center Pharmacy) to prevent blood clotting. Mice were then mounted on a 3D printed platform and fixed with bite and ear bars, after which they received 150 µl of D-luciferin via subcutaneous (s.c.) injection 10 min prior to treatment. BLI and X-ray was performed to localize the tumor and to guide the transducer to the tumor in the pons. A hydrophone was placed behind the ear of the mouse and coupled with a 1 MHz monoelement transducer using ultrasound gel. Microbubbles (SonoVue, Bracco International BV, Amsterdam) were prepared according to the manufacture's description. A 19 G needle was used to take up the microbubbles and fill up the catheter. Microbubbles were injected in two boli of 60 µl. Focused ultrasound was then performed at a frequency of 1.5 Hz to a total exposure time of 160 s, consisting of 40 repetitions over 6 points with a total 240 sonications. The safety of the procedure was monitored with passive caviation detection.

BBB opening

To ascertain optimal acoustic power in the HSJD-DIPG-07 xenograft model, different acoustic pressures were used, (Fig. 1: BBB opening). Mice received either 200 kPa ($n=3$) or 400 kPa ($n=3$). Directly after FUS, mice received Evans blue (100 µl, Sigma Aldrich, St. Louis, MO, USA). After 30 min mice were sacrificed and transcardially perfused with saline before brains were excised for analysis.

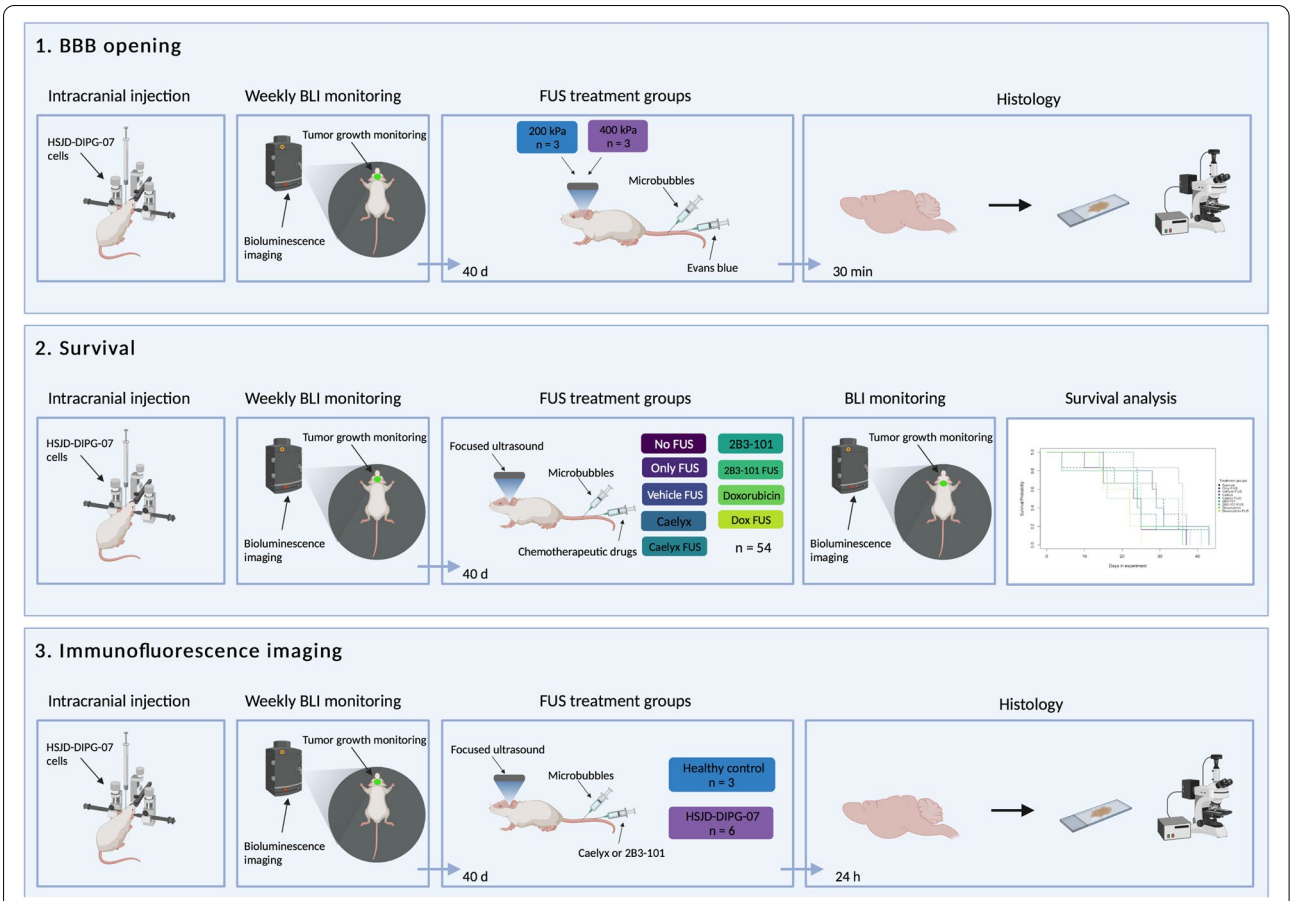

Fig. 1 Experimental design. BBB opening after FUS was determined in HSJD-DIPG-07 tumor-bearing mice which received 200 kPa ($n=3$) and 400 kPa ($n=3$) to observe the extent of BBB opening. Mice received 400 kPa during treatment in all subsequent experiments. Survival analysis was performed on HSJD-DIPG-07 xenograft models ($n=54$). Mice were regularly monitored with BLI and upon increase of the signal, mice received treatment with focused ultrasound. After treatment, mice were monitored and sacrificed at humane endpoints. Immunofluorescence histology was performed on non-tumor bearing mice ($n=3$) and tumor bearing mice (HSJD-DIPG-07) ($n=6$) to determine the presence of liposomal formulations of doxorubicin in the brain parenchyma. At 24 h after treatment mice were sacrificed and brains were frozen until analysis. (Created with Biorender)

Survival analysis

HSJD-DIPG-07 xenografts were established in 54 mice. Tumor engraftment was monitored with weekly BLI measurements (Fig. 1: survival). Upon increase of the BLI signal (indication of engraftment), at day 37 after implantation, mice were evenly stratified into nine groups of each 6 mice: (A) Control, (B) FUS only, (C) Vehicle liposomes + FUS, (D) doxorubicin + FUS, (E) systemic doxorubicin, (F) Caelyx® + FUS, (G) systemic Caelyx®, (H) 2B3-101 + FUS, and (I) systemic 2B3-101 ($n=6$ per group). At day 40, mice received 5 mg/kg doxorubicin (5 mg/kg, Vrije University Medical Center Pharmacy, Amsterdam, The Netherlands), Caelyx® (5 mg/kg, Vrije University Medical Center Pharmacy, Amsterdam, The Netherlands), 2B3-101 (5 mg/kg, kindly provided by dr. Pieter Gaillard) or control liposomes (PEG liposomes without doxorubicin) (kindly provided by prof. Gert Storm). The polyethylene glycol (PEG)-coated liposomal formulations of doxorubicin, Caelyx® and 2B3-101 as well as control liposomes were intravenously administered 60 min before sonoporation. Mice were regularly weighed and neurologically assessed. After treatment, BLI was performed twice a week for two weeks and followed by once a week to monitor tumor growth. At experimental endpoints, animals were deeply anaesthetized with a ketamine (2.4 mg, Alfasan Woerden, The Netherlands) and sedazine (0.24 mg, AST FARMA, Oudewater, The Netherlands) mixture and transcardially perfused with saline before brains were excised for analysis. In brief, once the animal was sedated and no reflexes were observed, an incision was made along the midline of the chest, and the resulting cavity was held open with retractors. A small incision was made to the left ventricle and right atrium and a blunt tip needle was then inserted

through the left ventricle into the anterior aorta and held in place with surgical clamps before 50 ml of saline was circulated through the vascular system using a syringe. Following perfusion, brains were excised and cut along the sagittal plane. One sagittal half was fixed in 4% formaldehyde (Merck, Darmstadt, Germany) and the other half was snap frozen in liquid nitrogen.

Histology and immunohistochemistry

PEG staining was done to visualize the localization of PEGylated liposomes (Fig. 1: immunofluorescence imaging). The staining was performed on both non-tumor bearing mice ($n=3$) and tumor bearing mice receiving Caelyx® ($n=3$) or 2B3-101 ($n=3$). Mice received focused ultrasound at 400 kPa. After 24 h, mice were transcardially perfused and brains were frozen in liquid nitrogen. Frozen tissue was cut at 5 µm. Tissue was fixed with ice cold methanol. Aldehyde groups were blocked with glycine (VWR, Fontenay-sous-Bois, France) after which the sections were incubated with primary anti-PEG-B-47 antibody (1:100) (Abcam, Cambridge, MA, USA) and rat anti-mouse CD31 (1:50) (BD Pharmingen, San Diego, CA, USA) in PBS containing 1% bovine serum albumin (Sigma Aldrich, St. Louis, MO, USA) overnight at RT. After washing, slices were incubated with Alexa Fluor goat anti-rabbit 488 and Alexa Fluor goat anti-rat 633 (Life technologies, Eugene, OR, USA) secondary antibodies for 30 min at room temperature (RT). Slices were then rinsed and mounted with Vectashield mounting medium containing DAPI (Vector laboratories, Burlingame, CA, USA) and kept in the dark until analyzed.

The following stainings were performed on tissue obtained from the BBB opening and survival studies. Formaldehyde fixed tissues were embedded in paraffin and sectioned into 5 µm slices using a microtome. Detailed observations of cellular and tissue structures in the brain were obtained by performing standard hematoxylin and eosin (HE) staining (Sigma Aldrich, St. Louis, MO, USA) on slide mounted brain samples. For paraffin embedded sections, slides were first deparaffinized in xylene, after which they were rehydrated in a series of alcohol baths. The sections were then stained with hematoxylin, rinsed and counterstained with eosin. Slices were dehydrated and mounted with mounting medium (Eukitt, Sigma Aldrich, Steinheim, Germany).

Vimentin staining was performed on paraffin embedded tissue by initially deparaffinizing and rehydrating sections, followed by blocking of endogenous peroxidases and permeabilization of the cell membrane with 0.3% peroxide (Merck, Darmstadt, Germany) in methanol (VWR, Fontenay-sous-Bois, France) for 30 min at RT. Antigen retrieval was performed using citrate buffer before incubation of the primary Mouse-α-Vimentin (1:4000, Monoclonal mouse anti-vimentin clone V9, Dako Denmark Glostrup, Denmark) for 1 h at RT. Vimentin was visualized with EnVision αM/αR and 3,3′-diaminobenzidine (DAB) (Dako, Glostrup, Denmark). The slices were counterstained with hematoxylin, dehydrated and mounted with a coverslip with mounting medium.

Blood vessels were visualized on both 5 µm frozen (HSJD-DIPG-07, $n=3$) and paraffin embedded tissue (non-tumor bearing control mice, $n=2$). Frozen tissue was fixed with 2% paraformaldehyde for 10 min. Slides were rinsed and aldehyde groups were blocked with glycine. Tissue was incubated with primary CD31 rat anti-mouse antibody (1:50) and rabbit anti-mouse laminin (1:500) (Abcam, Cambridge, MA, USA) overnight at RT. The following day, slides were washed and incubated with Alexa Fluor goat anti-rabbit 488 and Alexa Fluor goat anti-rat 633 secondary antibodies for 60 min at RT. After rinsing, tissue was mounted with Vectashield mounting medium containing DAPI and kept in the dark until analyzed. Paraffin embedded control tissue (mice without tumor) was deparaffinized and rehydrated before antigen retrieval with Tris–EDTA Buffer (10 mM Tris Base, 1 mM EDTA Solution, 0.05% Tween 20, pH 9.0). The tissue was then incubated with glycin for 10 min to block aldehyde groups. Slides were incubated with Lycopersicon esculentum (tomato) lectin (1:100, Vector laboratories, Burlingame, CA, USA) for 60 min at RT. Slides were rinsed and mounted with Vectashield mounting medium containing DAPI and stored in the dark.

Statistics

Survival analysis using Kaplan Meier and Log Rank test was performed in R (R Core Team (2017). R: A language and environment for statistical computing. R Foundation for Statistical Computing, Vienna, Austria. URL https://www.R-project.org/). Statistical significance was determined at $p<0.05$.

Results

BBB opening

To optimize safe drug delivery, different pressures (200 kPa and 400 kPa) were applied to determine the extent of BBB opening in HSJD-DIPG-07 xenograft-bearing mice. Figure 2A shows the detection of microbubbles after the first and second i.v. administration, followed by the rapid gradual clearance of the microbubbles from the vasculature (indicated by arrows). The frequency spectrum that monitored the stable and inertial cavitation of the microbubbles did not show inertial cavitation which can be observed by a sudden increase in noise floor (Fig. 2B). Rather, only a third harmonic was observed, indicative of stable cavitation. Treatment planning was

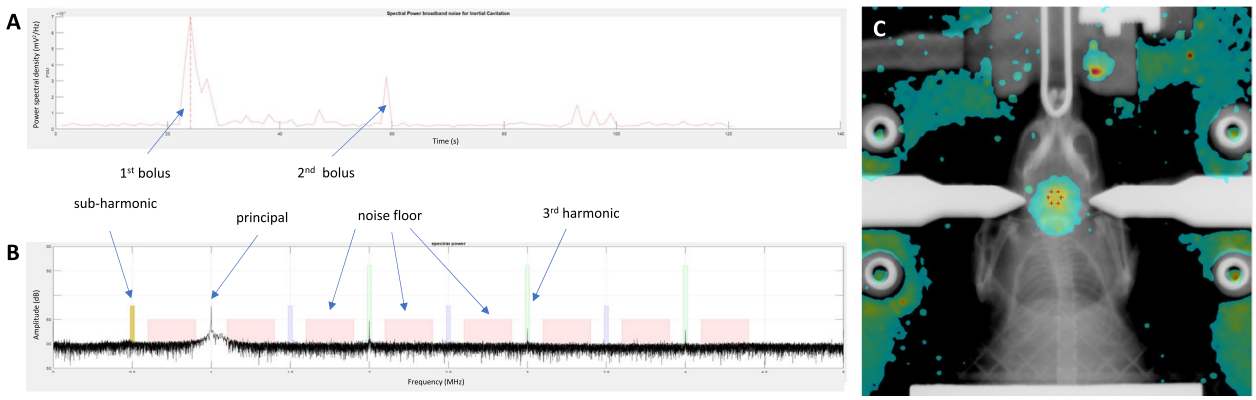

Fig. 2 Cavitation detection and targeting. **A** The acoustic energy of the microbubbles reflected to the transducer recorded over 240 sonications. The two boli ejections (blue arrows) can be observed followed by rapid clearance of the microbubbles. **B** Integrated power spectrum of the 3rd harmonic over time, indicating stable cavitation. No sudden increase in noise floor was observed. **C** Overlay of X-ray and BLI of mouse brain indicating the tumor in the red/yellow area. The target area is indicated with a hexagon (6 red dots)

performed using a combination of X-ray and BLI, targeting the pontine region (Fig. 2C) [25].

Both pressures were well tolerated with no observation of bleeding or tissue damage, as shown with histology (Fig. 3). Moreover, the image-guided targeting of FUS resulted in the local opening of the BBB in the pontine region, as visualized with Evans Blue, the golden standard to show BBB opening. However, we observed that the extent of BBB opening following 200 kPa was remarkably lower, exemplified by lower Evans Blue extravasation and inadequate coverage of the tumor region defined by human vimentin staining, 400 kPa was chosen for treatment (Fig. 3).

Survival analysis

BLI signal exponentially increased at day 37 after i.c. injections (Fig. 4A). Although BLI is not an exact measure for tumor size, it is a reliable indication of tumor growth and hence this was used to stratify mice into nine groups: (A) Control, (B) FUS only, (C) Vehicle liposomes + FUS, (D) systemic doxorubicin + FUS, (E) systemic doxorubicin, (F) Caelyx® + FUS, (G) systemic Caelyx®, (H) 2B3-101 + FUS, and (I) systemic 2B3-101 ($n = 6$ per group). At day 40, mice were treated and received 5 mg/kg doxorubicin, 5 mg/kg Caelyx®, 5 mg/kg 2B3-101 or 5 mg/kg control liposomes. Mice maintained a stable weight directly after treatment, although weight decline was observed over time that correlated with increasing tumor growth measured with BLI (Supplemental Fig. 1). After treatment, mice underwent BLI twice weekly for two weeks and thereafter once a week until humane endpoint was reached. BLI monitoring did not reveal a decrease in signal intensity after treatment (Supplemental Fig. 2),

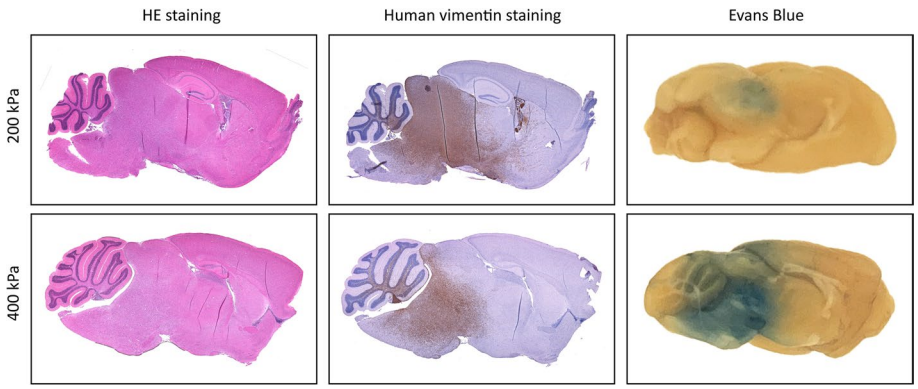

Fig. 3 Sagittal brain sections of FUS treated HSJD-DIPG-07 xenograft-bearing mice showing safety and BBB opening. Left: HE stainings indicating no tissue damage after FUS at 200 and 400 kPa. Middle: Human vimentin staining showing the diffuse growth pattern of HSJD-DIPG-07 xenograft. Right: Evans Blue extravasation after FUS showing an overlap with the human vimentin (tumor) staining at 400 kPa while at 200 kPa the tumor area is not covered

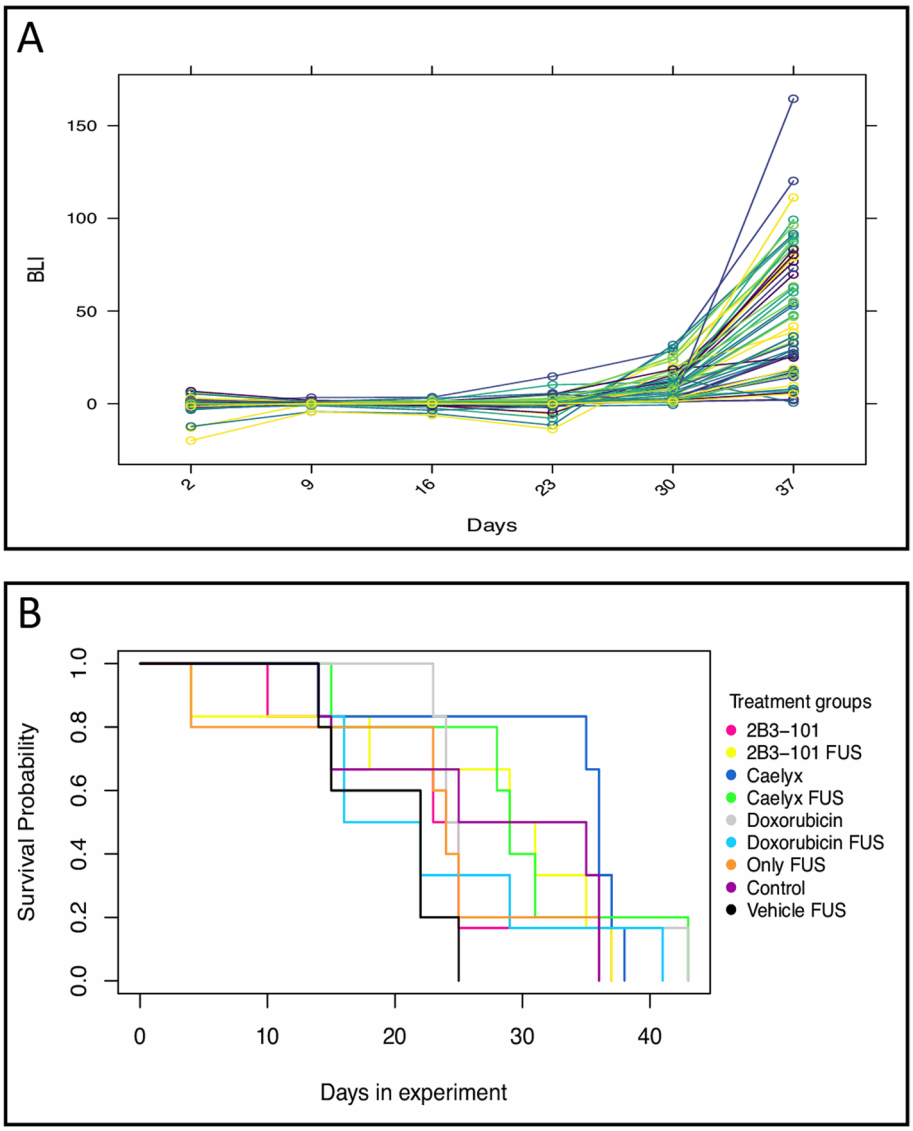

Fig. 4 BLI monitored tumor engraftment and survival following treatment. **A** Weekly BLI (photon/sec/m2) monitoring as a measure of tumor engraftment. The mean intensity of the background was subtracted from the tumor BLI. Exponential growth was observed 37 days after tumor implantation. **B** Survival analysis (Kaplan–Meier curve) of the different treatment groups. Day 0 is the start of treatment. "Days in experiment" represents the number of days after treatment. Differences in groups ($n=6$ mice per group) were not statistically significant ($p=0.3$)

which indicates that tumor growth was not stalled or reduced. The survival curves of the different treatment groups overlap. Survival analysis, using Kaplan Meier and Log Rank, showed no significant differences between the different treatment groups ($p=0.3$, Fig. 4B and Supplemental Fig. 3).

Liposome extravasation into the brain parenchyma

Since no significant difference in survival was observed, the presence of doxorubicin-loaded liposomes in the vasculature and brain parenchyma was investigated with immunofluorescence stainings. Therefore, sagittal slices of mouse brain were incubated with an anti-PEG antibody to determine the local extravasation of liposomes in the pontine area (Fig. 5). In non-tumor bearing mice (control), PEGylated liposomes were clearly extravasated and retained in the pontine area at 24 h after FUS treatment. PEGylated liposomes were observed in the brain parenchyma, in close vicinity of the blood vessels, resulting in only a partial exposure. However, two out of three brains of tumor bearing mice treated with Caelyx® and FUS stained positive for liposomes in the blood vessels

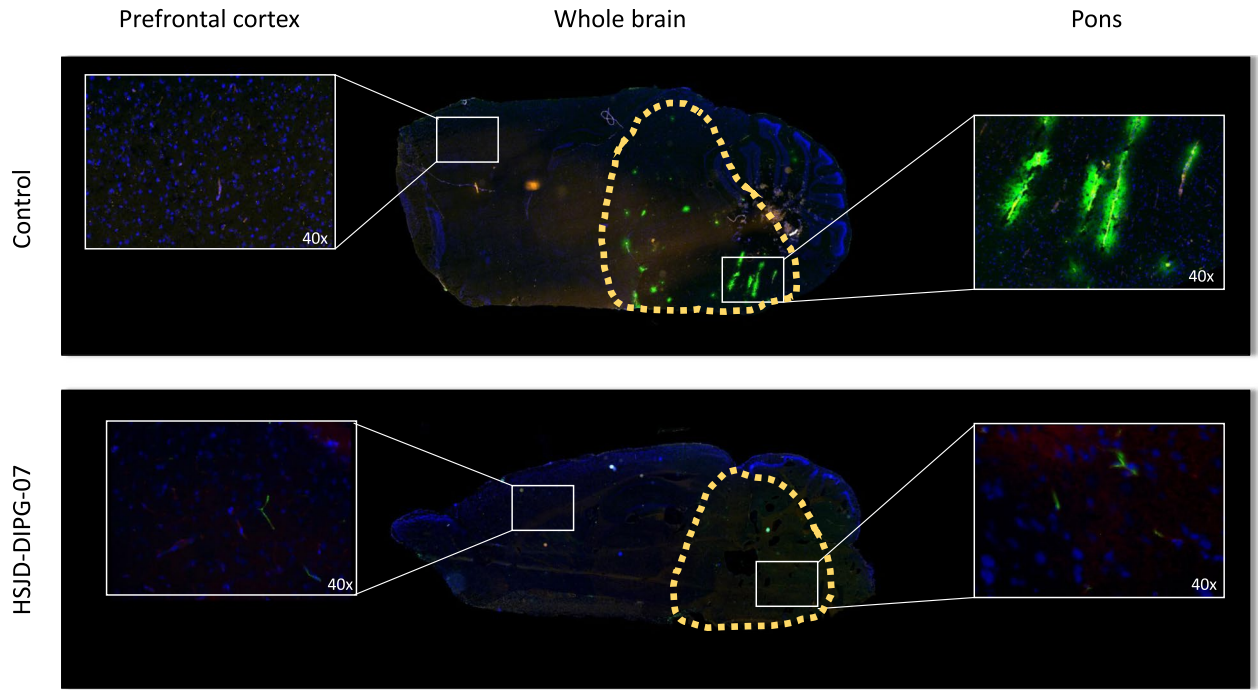

Fig. 5 Immunofluorescent PEG staining on sagittal slices of FUS-treated mouse brains. A positive staining of liposomes (in green) was detected in the pontine region of control (non-tumor bearing mice) (upper panel) who received Caelyx®. The pontine/tumor area delineated with a yellow dotted line. In contrast, only few liposomes were observed in the blood vessels of the HSJD-DIPG-07 xenograft model that received Caelyx® (lower panel). In both panels endothelial cells are indicated in red (CD31 staining), nuclei in blue (DAPI)

after 24 h but not in the brain parenchyma (Supplemental Fig. 4). One Caelyx® FUS and three 2B3-101 FUS-treated animals stained negative for PEG. The control groups also stained negative for liposomes.

Discussion

Current standard treatment for DIPG patients consist of radiotherapy in combination with adjuvant chemotherapy, resulting in a median overall survival of 11 months [1, 26]. However, after years of preclinical and clinical testing of new therapeutic approaches, the overall survival of DIPG patients remains unchanged [1, 27]. It is thought that most drugs do not reach and maintain high enough drug concentrations in the tumor area and thus result in a low efficacy in patients [28, 29]. Various formulations of doxorubicin have been used in phase I/II studies in both adult glioma and pediatric high-grade glioma population without clear benefit [30–32]. Most of these clinical studies have been initiated by promising in vitro results for many interesting drug candidates but in vivo do not show the same efficacy. One of the reasons could be that drug concentrations are low. The BBB, which is believed to remain intact in patients with DIPG, limits the exposure of the drugs to the brain [4, 5]. Since, only small molecules (< 500 Da) can enter the brain parenchyma, only a limited number of drugs are suitable for adjuvant treatment in DIPG [6]. As most drugs that have been developed do not readily cross the BBB, drug delivery methods are needed to circumvent the BBB and allow these drugs to enter the parenchyma [7].

Microbubble-mediated FUS has been used successfully in several orthotopic models. This drug delivery method has been shown to specifically target the tumor area and locally increase drug concentrations [33, 34]. More importantly, FUS is a minimally invasive procedure with fast recovery times and no serious side effects. To date, FUS has been successfully used in preclinical glioma models using temozolomide, bevacizumab, carboplatin, BCNU, etoposide, and doxorubicin [18, 33–40]. In both a 9-L glioma rat model as well as a U87 mouse model temozolomide significantly increased median survival [33, 38]. Bevacizumab combined with FUS showed an increase in median survival in a U87 mouse model and normalization of the tumor vasculature was observed due to the bevacizumab-related block of vascular endothelial growth factor (VEGF) [34, 41]. FUS with carboplatin also showed improvement in survival in a U87 mouse model but had a non-significant result in a patient-derived cell line (6240 LN) [39]. Furthermore, BCNU and etoposide showed a significant survival benefit, respectively in C6

glioma rats and a syngeneic mouse model (MGPP3 harboring PDGF^{+}, Pten$^{-/-}$, P53$^{-/-}$) [37, 40]. However, the compounds that have been studied most in adult glioma models in combination with FUS are doxorubicin and liposomal doxorubicin [36, 42, 43]. Combining free doxorubicin with FUS resulted in an increase of drug concentration in the brain and improved overall survival in SMA 560 and GL261 glioma mouse models [36]. Furthermore, FUS in combination with a liposomal formulation of doxorubicin has shown improvement of survival in a 9L rat glioma model [18, 44]. However, here improvement in survival was accompanied by severe side effects common to doxorubicin such as skin toxicity, impaired activity, damage to surrounding brain tissue, tissue loss at the tumor site, and intratumoral hemorrhage [44].

Since FUS has been successful in treating different adult glioma models, we aimed to explore the use of this technique for the treatment of pediatric DIPG in a preclinical animal model. In vitro, doxorubicin was found to be effective on primary cell cultures, including HSJD-DIPG-07 [17, 45]. Since doxorubicin was found to be effective in vitro against DIPG cell lines and FUS in combination with (liposomal) doxorubicin has shown a survival benefit in glioma xenograft models, doxorubicin could be a good candidate for treatment of preclinical DIPG mouse model [17]. Ishida and colleagues recently showed that while FUS was able to enhance delivery of free doxorubicin into the brain, the combined use did not have the desired improvement in survival in a DIPG xenograft model [14]. Initially, Ishida and colleagues used 5 mg/kg of doxorubicin in vivo, which led to severe toxicity. Subsequently, a cumulative dose of 3 mg/kg (1.5 mg/kg weekly over 2 weeks) was used. However, unexpected toxicity was once again observed while survival benefits were not realized [14].

We hypothesized that the use of FUS with various formulations of PEGylated liposomal doxorubicin would reduce toxicity and expose the tumor for a prolonged period of time to doxorubicin. Contrary to Ishida et al., 5 mg/kg of free doxorubicin did not result in severe toxicity in our mouse model. Previous experiments showed that 5 mg/kg doxorubicin was tolerated and not toxic to the animals (Sewing et al., and data not shown) [17]. However, we observed that longer treatment times with FUS (>20 min) resulted in poor recovery and increased weight loss. Since MRI-guided FUS as used by Ishida has a longer treatment time than the BLI image-guided FUS we used in our study [25]. The use of doxorubicin in combination with MRI-guided FUS with long treatment times might have resulted in limiting toxicities. Besides differences in treatment times, in our study mice also received additional nutritional food supplement to aid recovery. Furthermore, the used mouse strain (NOD scid gamma (NSG) vs nude-foxn1^{nu}), and tumor model (SU-DIPG-17 vs DIPG-HSJD-07) differed in these studies, as well as the method to visualize tumor growth.

Since PEGylated liposomes can be visualized with immunofluorescence, we stained the liposomes in both healthy controls and xenograft tissue to confirm delivery into the brain. Remarkably, liposomes were clearly observed in non-tumor bearing mice (control) tissue but not in HSJD-DIPG-07 brain tissue. In only two mice treated with Caelyx® and FUS we observed areas with PEGylated liposomes within the blood vessels but not in the brain parenchyma at 24 h after treatment. These liposomes were not limited to the FUS treated area, which therefore might indicate local areas of poor cardiac perfusion. Hence, the lack of survival benefit might be a result of the lack of liposomes in the brain parenchyma, as observed already 24 h after treatment. The absence of liposomes might be caused by a high intratumoral pressure preventing accumulation of liposomes in the brain parenchyma [46]. Furthermore, the morphology and functionality of endothelial cells might be altered in the presence of a tumor, which can have a negative effect on liposomal binding in the endocytosis/transcytosis pathway, thus preventing liposomes to cross the BBB [47, 48]. Moreover, Alli et al. showed a 50-fold increase in doxrobucin concentration upon FUS treatment in non-tumor bearing mice, while Ishida et al. showed only a four-fold increase in a DIPG model [16, 49]. Therefore, the lack of accumulation of doxorubicin and doxorubicin liposomes might be intrinsic to the presence of a tumor or certain tumor type. These hypotheses should be further explored to explain the absence of liposomes 24 h after FUS. However, the analysis of liposomes in the brain is problematic since conventional analytical methods such as mass spectrometry or high-pressure liquid chromatography (HPLC) cannot distinguish between blood vessel and brain parenchyma, consequently making it impossible to determine the exact location of the liposomes. Additionaly, liposomes are packed with multiple doxorubicin molecules and therefore determination of doxorubicin concentration is not a good measure to calculate the concentration of the drug in the brain. Microdialysis would have enabled us to determine the presence of liposomes over time in the brain, but this technique requires a metal canula that will interfere with FUS and therefore was not suited for our experiments. Visualisation of liposomes in the brain and tumour regions following FUS treatment has also been unachievable for other groups, which relied heavily on HPLC and MS in showing doxorubicin concentration rather than presence of liposomes [18, 43].

Another possible explanation for the lack of efficacy observed in both our study and in Ishida et al. are the

pharmacokinetics and –dynamics of (liposomal) doxorubicin in rodents, in relationship to the exposure needed to reach an effective local tissue area under the curve (AUC) in vivo that can compare with in vitro IC50. For the cell line used in our study, the IC50 was previously ascertained to be 40 nM at 96 h. In published data, after administration of 5 mg/kg doxorubicin in rodents a Cmax of 10 µg/ml (18.4 µM) was reached just after injection but swiftly decreased to plasma concentrations between 0.1 and 0.01 µg/ml at 72 h, corresponding to 184 nM and 18.4 nM respectively [50]. Alli et al. found a local brainstem tissue concentration of 824 nM, two hours after FUS and injection of 5 mg/kg doxorubicin in NGS mice [16]. If and how local tissue concentrations stay above the in vitro AUC can be debated. Potentially, the plasma wash-out goes hand in hand with decreasing local drug concentrations after FUS. With regard to the pharmacokinetics of liposomal formulations, important differences are observed compared to free doxorubicin, with an up to 2.6 – 6.8 increased plasma AUC [51]. Of note however in this respect is the fact that this AUC mainly reflects the presence of encapsulated doxorubicin, which is released over a longer time frame, with free drug slowly released from the liposomes, long after the BBB has closed after FUS. Furthermore, in patients often lower single doses of doxorubicin are administered, ranging between 1 – 1.6 mg/kg, which further limits the translatability of our study towards clinical trials. Yet, a clinical study that evaluates the safety of Caelyx® in combination with transcranial MRI-guided FUS for adult brain tumor patients is currently planned as a basis for later studies to evaluate clinical efficacy (NCT02343991). Here, we aimed to compare the effects of Caelyx® and 2B3-101 – which both have been approved for clinical use – in combination with FUS to determine if there would be a treatment benefit of any of those compounds. 2B3-101 has been designed specifically for the treatment of brain tumor patients and has been shown to have a 5-times higher drug delivery into the brain than Caelyx® (in the absence of FUS) [52], while the slightly smaller size of Caelyx® might enhance brain distribution after passing the BBB. However, since in our experiments no difference in survival was observed and both liposomes could not be visualized in the treated animals, we cannot draw any conclusions about the difference between Caelyx® and 2B3-101 after FUS treatment. Regarding the programmed clinical trial, however, it should be noted that in various preclinical studies there is a clear difference in survival benefit between adult glioma and paediatric DIPG models. Both etoposide and doxorubicin have been used in preclinical models of glioma and DIPG [14, 36, 37, 53]. While etoposide and doxorubicin prolonged survival in adult glioma models, these compounds did not improve survival in preclinical models of DIPG, even after multiple treatments [37, 53]. This raises the question why is there a difference in efficacy, especially since etoposide was used in the same tumor model, with the only difference being the anatomical location of implantation. While there is little information on the permeability of the heterogenous BBB, there are indications that the BBB in the pontine region is more tightly regulated than other areas of the brain [4]. This might result in different BBB opening dynamics with FUS. Furthermore, we observed that the liposomes do not diffuse far into the tissue and remain in the vicinity of the blood vessels exposing only a small pontine area to the drug. In a recent study in our group, we found that the number of blood vessels are reduced in DIPG patients compared to healthy controls [54]. This would limit the exposure of drugs after treatment with FUS due to the low blood vessel density. To design an effective treatment for DIPG, we therefore hypothesize that a combination of FUS with other modalities could be beneficial. For example, low-freqency FUS has been shown to induce an immune response, such as an increased expression of pro-inflamatory cytokines, chemokines and infiltration of immune cells in the brain parenchyma [55]. However, more research is needed to investigate such combinations, as we could not determine the effects of FUS on the immune system in our (immune-deficient) xenografts. Of note, the HSJD-DIPG-07 mouse model used in our experiments showed a relatively high number of vessels compared to healthy controls (392.5 blood vessels/nm [2] versus 219.3 blood vessels/ nm [2] respectively), and therefore blood vessel count does most likely not explain the ineffectiveness of the treatment described here. As such, there are still a lot of uncertainties before FUS can be translated into the clinic. Future research should investigate the exact reason why FUS in combination with various formulations of doxorubicin has been unsuccessful. Pharmacokinetic considerations are of high importance in the choice of drugs repurposed for FUS in this respect.

Conclusion

In conclusion, FUS is a non-invasive technique that has been successfully used in preclinical glioma models. Here, we report a third study investigating FUS for the treatment of DIPG that shows safety, but does not show survival benefit after treatment with doxorubicin, 2B3-101, and Caelyx®. Further studies are needed to investigate the reason why FUS has a different response in DIPG xenograft models in order to translate into better treatments for this deadly pediatric brain cancer.

Abbreviations

DIPG: Diffuse intrinsic pontine glioma; BBB: Blood-brain barrier; FUS: Focused ultrasound; BLI: Bioluminescence imaging; CED: Convection enhanced delivery;

GSH: Glutathione; TSM: Tumor stem medium; bFGF: Basic fibroblast growth factor; EGF: Epidermal growth factor; PDGF: Platelet-derived growth factor; STR: Short tandem repeat; PBS: Phosphate buffered saline; VU: Vrije University; i.p.: Intraperitoneally; ROI: region of interest; s.c.: Subcutaneous; PEG: Polyethylene glycol; HE: Hematoxylin and eosin; RT: Room temperature; DAB: 3,3′-Diaminobenzidine; VEGF: Vascular endothelial growth factor; NSG: NOD scid gamma; HPLC: High-pressure liquid chromatography; AUC: Area under the curve.

Supplementary Information

The online version contains supplementary material available at https://doi.org/10.1186/s41231-022-00115-7.

Additional file 1: Figure S1. Weight registration, Weight (grams, y-axis) was regularly monitored to assess animal well-being over time (days, x-axis). Overall mice weight remained stable around the treatment day, indicated by a red dotted line. With increasing tumor growth, weight also decreased. **Figure S2.** BLI monitoring, BLI was measured twice a week for two weeks after treatment followed by once a week until humane endpoint was reached. For all mice, BLI signal did not decline after treatment, indicating tumor growth. Notably, in several cases BLI signal drastically dropped at humane endpoint. Dotted red line indicates time of treatment. **Figure S3.** Survival Analysis. Separated graphs from Figure 4 (Controls vs. Treatment). Day 0 is the start of treatment. "Days in experiment" represents the number of days after treatment. Figure 3A displays the survival curves of the control, vehicle FUS, and only FUS (p =0.2). Here, graphs overlap indicating no difference between the control groups. The same holds true for the treatment groups displayed in Figure 3B (survival curves of control, doxorubicin with FUS, and doxorubicin)($p = 0.7$), 3C (control, Caelyx® with FUS, and Caelyx®)($p = 0.5$) and 3D (control, 2B3-101 with FUS, and 2B3-101)($p = 0.9$). **Figure S4.** Immunofluorescent (IF) staining on sagittal slices of mouse brains. A: IF of blood vessels (CD31 in red) and pegylated liposomes (anti-PEG in green) did not show the presence of liposomes 24 h after treatment except for mouse 1 and mouse 2 treated with Caelyx® and FUS. Yellow area indicates the tumor area. B: Enlarged picture shows the presence of Caelyx® liposomes in the cortex outside of the sonoporated area.

Acknowledgements
We would like to thank dr. Pieter Gaillard for providing 2B3-101 and prof. Gert Storm for providing control liposomes. Furthermore, we would like to thank ing. J. Horstik and ir. M. van der Boom for their help with 3D printing.

Authors' contributions
Conceptualization, RH, JB, PG and EH.; methodology, RH, JB and EH; validation, RH and JB; formal analysis, RH and JB; investigation, RH, JB, GS, PG and PMW.; resources, MR; data curation, RH; writing—original draft preparation, RH, JB and EH; writing—review and editing, EH, PG, GS, GJK, DGV and MR; visualization, RH; supervision, GJK and EH; project administration, DGV, GJK and EH.; funding acquisition, EH and DGV. All authors have read and agreed to the published version of the manuscript.

Funding
This research was funded by KWF-STW (Project number: 15184) and KiKa (Children Cancer Free Foundation).

Availability of data and materials
All data are available upon request.

Declarations

Ethics approval and consent to participate
All animal studies were reviewed and approved by the committee on animal experimentation of the Vrije University (AVD114002017841). Animal experiments were conducted in accordance with the Dutch law on animal experimentation.

Consent for publication
Not applicable.

Competing interests
The authors declare no conflict of interest.

Author details
[1]Princess Máxima Center for Pediatric Oncology, Heidelberglaan 25, 3584 CS Utrecht, The Netherlands. [2]Pediatric Oncology, Amsterdam UMC, Vrije Universiteit Amsterdam, Cancer Center Amsterdam, De Boelelaan, 1117-1118, 1081 HV Amsterdam, The Netherlands. [3]2-BBB Medicines BV, J.H, Oortweg 19, 2333 CH Leiden, The Netherlands. [4]Department of Pharmaceutics, Faculty of Science, Utrecht University, Universiteitsweg 99, 3584 CG Utrecht, The Netherlands. [5]Department of Biomaterials, Science and Technology, Faculty of Science and Technology, University of Twente, Drienerlolaan 5, 7522 NB Enschede, The Netherlands. [6]Department of Radiology, Utrecht University, Heidelberglaan 8, 3584 CS Utrecht, The Netherlands.

Received: 3 January 2022 Accepted: 26 March 2022
Published online: 18 April 2022

References

1. Hoffman LM, et al. Clinical, radiologic, pathologic, and molecular characteristics of long-term survivors of diffuse intrinsic Pontine Glioma (DIPG): a collaborative report from the international and European Society for Pediatric Oncology DIPG registries. J Clin Oncol. 2018;36(19):1963–72.
2. Wagner S, et al. Treatment options in childhood pontine gliomas. J Neurooncol. 2006;79(3):281–7.
3. Gokce-Samar Z, et al. Pre-radiation chemotherapy improves survival in pediatric diffuse intrinsic pontine gliomas. Childs Nerv Syst. 2016;32(8):1415–23.
4. McCully CM, et al. Model for concomitant microdialysis sampling of the pons and cerebral cortex in rhesus macaques (Macaca mulatta). Comp Med. 2013;63(4):355–60.
5. Warren KE. Beyond the blood: brain barrier: the importance of central nervous system (CNS) pharmacokinetics for the treatment of CNS tumors, including diffuse intrinsic pontine glioma. Front Oncol. 2018;8:239.
6. Pardridge WM. The blood-brain barrier: bottleneck in brain drug development. NeuroRx. 2005;2(1):3–14.
7. Haumann R., Videira J. C. Kaspers, G. J. van Vuurden D. G. & Hulleman E. Overview of Current Drug Delivery Methods Across the Blood–Brain Barrier for the Treatment of Primary Brain Tumors. CNS drugs. 2020;34(11):1121–31.
8. Patel MM, Patel BM. Crossing the blood–brain barrier: recent advances in drug delivery to the brain. CNS Drugs. 2017;31(2):109–33.
9. Agarwal S, et al. Active efflux of Dasatinib from the brain limits efficacy against murine glioblastoma: broad implications for the clinical use of molecularly targeted agents. Mol Cancer Ther. 2012;11(10):2183–92.
10. Hynynen K, McDannold N, Vykhodtseva N, Jolesz FA. Noninvasive MR imaging–guided focal opening of the blood-brain barrier in rabbits. Radiology. 2001;220(3):640–6.
11. McDannold N, Arvanitis CD, Vykhodtseva N, Livingstone MS. Temporary disruption of the blood–brain barrier by use of ultrasound and microbubbles: safety and efficacy evaluation in rhesus macaques. Can Res. 2012;72(14):3652–63.
12. Carpentier A, et al. Clinical trial of blood-brain barrier disruption by pulsed ultrasound. Sci trans med. 2016;8(343):343re342-343re342.
13. Mainprize T, et al. Blood-Brain Barrier Opening in Primary Brain Tumors with Non-invasive MR-Guided Focused Ultrasound: A Clinical Safety and Feasibility Study. Sci Rep. 2019;9(1):321.
14. Ishida J, et al. MRI-guided focused ultrasound enhances drug delivery in experimental diffuse intrinsic pontine glioma. J Control Release. 2021;330:1034–45.
15. Idbaih A, et al. Safety and feasibility of repeated and transient blood–brain barrier disruption by pulsed ultrasound in patients with recurrent glioblastoma. Clin Cancer Res. 2019;25(13):3793–801.
16. Alli S, et al. Brainstem blood brain barrier disruption using focused ultrasound: A demonstration of feasibility and enhanced doxorubicin delivery. J Control Release. 2018;281:29–41.

17. Sewing ACP, et al. Preclinical evaluation of convection-enhanced delivery of liposomal doxorubicin to treat pediatric diffuse intrinsic pontine glioma and thalamic high-grade glioma. J Neurosurg Pediatr. 2017;19(5):518–30.
18. Treat LH, McDannold N, Zhang Y, Vykhodtseva N, Hynynen K. Improved anti-tumor effect of liposomal doxorubicin after targeted blood-brain barrier disruption by MRI-guided focused ultrasound in rat glioma. Ultrasound Med Biol. 2012;38(10):1716–25.
19. Rafiyath S. M., et al. Comparison of safety and toxicity of liposomal doxorubicin vs. conventional anthracyclines: a meta-analysis. Exp Hematol Oncol. 2012;1(1):10.
20. Gaillard PJ, et al. Pharmacokinetics, brain delivery, and efficacy in brain tumor-bearing mice of glutathione pegylated liposomal doxorubicin (2B3–101). PloS one. 2014;9(1):e82331.
21. Birngruber T, et al. Enhanced doxorubicin delivery to the brain administered through glutathione PEGylated liposomal doxorubicin (2B3-101) as compared with generic Caelyx,®/Doxil®—a cerebral open flow microperfusion pilot study. J Pharm Sci. 2014;103(7):1945–8.
22. Gabizon A, Shmeeda H, Barenholz Y. Pharmacokinetics of pegylated liposomal doxorubicin. Clin Pharmacokinet. 2003;42(5):419–36.
23. Meel MH, Metselaar DS, Waranecki P, Kaspers GJL, Hulleman E. An efficient method for the transduction of primary pediatric glioma neurospheres. MethodsX. 2018;5:173–83.
24. Thomale U, et al. Neurological grading, survival, MR imaging, and histological evaluation in the rat brainstem glioma model. Childs Nerv Syst. 2009;25(4):433–41.
25. Haumann R, et al. A High-Throughput Image-Guided Stereotactic Neuronavigation and Focused Ultrasound System for Blood-Brain Barrier Opening in Rodents. J Vis Exp. 2020. https://doi.org/10.3791/61269(161).
26. Wagner S, et al. Treatment options in childhood pontine gliomas. J Neurooncol. 2006;79(3):281–7.
27. Hargrave D, Bartels U, Bouffet E. Diffuse brainstem glioma in children: critical review of clinical trials. Lancet Oncol. 2006;7(3):241–8.
28. Cohen KJ, et al. Temozolomide in the treatment of children with newly diagnosed diffuse intrinsic pontine gliomas: a report from the Children's Oncology Group. Neuro Oncol. 2011;13(4):410–6.
29. van Zanten SEV, et al. A phase I/II study of gemcitabine during radiotherapy in children with newly diagnosed diffuse intrinsic pontine glioma. J Neurooncol. 2017;135(2):307–15.
30. Chastagner P, et al. Phase I study of non-pegylated liposomal doxorubicin in children with recurrent/refractory high-grade glioma. Cancer Chemother Pharmacol. 2015;76(2):425–32.
31. Marina NM, et al. Dose escalation and pharmacokinetics of pegylated liposomal doxorubicin (Doxil) in children with solid tumors: a pediatric oncology group study. Clin Cancer Res. 2002;8(2):413–8.
32. Wagner S, et al. Pegylated-liposomal doxorubicin and oral topotecan in eight children with relapsed high-grade malignant brain tumors. J Neurooncol. 2008;86(2):175–81.
33. Liu H-L, et al. Pharmacodynamic and therapeutic investigation of focused ultrasound-induced blood-brain barrier opening for enhanced temozolomide delivery in glioma treatment. PloS one. 2014;9(12):e114311.
34. Liu H-L, et al. Focused ultrasound enhances central nervous system delivery of bevacizumab for malignant glioma treatment. Radiology. 2016;281(1):99–108.
35. Bunevicius A, McDannold NJ, Golby AJ. Focused ultrasound strategies for brain tumor therapy. Operative Neurosurgery. 2020;19(1):9–18.
36. Kovacs Z, et al. Prolonged survival upon ultrasound-enhanced doxorubicin delivery in two syngenic glioblastoma mouse models. J Control Release. 2014;187:74–82.
37. Wei H-J. et al. Focused Ultrasound-Mediated Blood-Brain Barrier Opening Increases Delivery and Efficacy of Etoposide for Glioblastoma Treatment. Int J Radiat Oncol Biol Physics. 2021;110.2:539–50.
38. Wei K-C, et al. Focused ultrasound-induced blood–brain barrier opening to enhance temozolomide delivery for glioblastoma treatment: a preclinical study. PloS one. 2013;8(3):e58995.
39. Dréan A, et al. Temporary blood–brain barrier disruption by low intensity pulsed ultrasound increases carboplatin delivery and efficacy in preclinical models of glioblastoma. J Neurooncol. 2019;144(1):33–41.
40. Liu H-L, et al. Blood-brain barrier disruption with focused ultrasound enhances delivery of chemotherapeutic drugs for glioblastoma treatment. Radiology. 2010;255(2):415–25.
41. Zhao C, Wang H, Xiong C, Liu Y. Hypoxic glioblastoma release exosomal VEGF-A induce the permeability of blood-brain barrier. Biochem Biophys Res Commun. 2018;502(3):324–31.
42. Lin Y-L, Wu M-T, Yang F-Y. Pharmacokinetics of doxorubicin in glioblastoma multiforme following ultrasound-Induced blood-brain barrier disruption as determined by microdialysis. J Pharm Biomed Anal. 2018;149:482–7.
43. Sun T, et al. Closed-loop control of targeted ultrasound drug delivery across the blood–brain/tumor barriers in a rat glioma model. Proc Natl Acad Sci. 2017;114(48):E10281–90.
44. Aryal M, Vykhodtseva N, Zhang Y-Z, Park J, McDannold N. Multiple treatments with liposomal doxorubicin and ultrasound-induced disruption of blood–tumor and blood–brain barriers improve outcomes in a rat glioma model. J Control Release. 2013;169(1–2):103–11.
45. Ung C, et al. Doxorubicin-Loaded Gold Nanoarchitectures as a Therapeutic Strategy against Diffuse Intrinsic Pontine Glioma. Cancers. 2021;13(6):1278.
46. Harward S, Farber SH, Malinzak M, Becher O, Thompson EM. T2-weighted images are superior to other MR image types for the determination of diffuse intrinsic pontine glioma intratumoral heterogeneity. Childs Nerv Syst. 2018;34(3):449–55.
47. Hofman P, van Blijswijk BC, Gaillard PJ, Vrensen GF, Schlingemann RO. Endothelial cell hypertrophy induced by vascular endothelial growth factor in the retina: new insights into the pathogenesis of capillary nonperfusion. Arch Ophthalmol. 2001;119(6):861–6.
48. Witmer AN, van Blijswijk BC, van Noorden CJ, Vrensen GF, Schlingemann RO. In vivo angiogenic phenotype of endothelial cells and pericytes induced by vascular endothelial growth factor-A. J Histochem Cytochem. 2004;52(1):39–52.
49. Ishida J, et al. MRI-guided focused ultrasound enhances drug delivery in experimental diffuse intrinsic pontine glioma. J Control Release. 2020;330(10):1034–45.
50. Lee JB, et al. Interspecies prediction of pharmacokinetics and tissue distribution of doxorubicin by physiologically-based pharmacokinetic modeling. Biopharm Drug Dispos. 2020;41(4–5):192–205.
51. Lu W-L, et al. A pegylated liposomal platform: pharmacokinetics, pharmacodynamics, and toxicity in mice using doxorubicin as a model drug. J Pharmacol Sci. 2004;95(3):381–9.
52. Brandsma D, et al. Phase 1/2a study of glutathione pegylated liposomal doxorubicin (2b3–101) in patients with brain metastases (BM) from solid tumors or recurrent high grade gliomas (HGG). Annals Oncol. 2014;25:iv157.
53. Englander ZK, et al. Focused ultrasound mediated blood–brain barrier opening is safe and feasible in a murine pontine glioma model. Sci Rep. 2021;11(1):1–10.
54. El-Khouly FE, et al. The neurovascular unit in diffuse intrinsic pontine gliomas. Free Neuropathology. 2021;2:17–17.
55. Kim C, Lim M, Woodworth GF, Arvanitis CD. The roles of thermal and mechanical stress in focused ultrasound-mediated immunomodulation and immunotherapy for central nervous system tumors. J Neurooncol. 2022;1-16.

Publisher's Note